KSÜ Tarım ve Doğa Derg 28 (2), 335-350, 2025
KSU J. Agric Nat 28 (2), 335-350, 2025
DOI:10.18016/ksutarimdoga.vi.1591728

Molecular Docking Studies and Biological Activities of Chalcones Targeting Acetylcholinesterase, and Carbonic Anhydrase Isoenzymes

Mehtap TUGRAK SAKARYA[1✍], Halise Inci GUL[2], Yusuf SERT[3], Hulya AKINCIOGLU[4], Ilhami GULCIN[5], Mustafa GUL[6]

[1]Department of Pharmaceutical Chemistry, Faculty of Pharmacy, Tokat Gaziosmanpasa University, Tokat, Türkiye, [2]Department of Pharmaceutical Chemistry, Faculty of Pharmacy, Ataturk University, Erzurum, Türkiye, [3]Department of Motor Vehicles and Transportation Technologies, SorgunVocational High School, Yozgat Bozok University, Yozgat, Türkiye, [4]Department of Chemistry, Faculty of Science and Arts, Agri Ibrahim Cecen University, Agri, Türkiye [5]Department of Chemistry, Faculty of Science, Ataturk University, Erzurum, Türkiye, [6]Department of Physiology, Faculty of Medicine, Ataturk University, Erzurum, Türkiye

[1]https://orcid.org/0000-0002-6535-6580, [2]https://orcid.org/0000-0001-6164-9602, [3]https://orcid.org/0000-0001-8836-8667
[4]https://orcid.org/0000-0001-5453-0953, [5]https://orcid.org/0000-0001-5993-1668, [6]https://orcid.org/0000-0002-0042-890X
✉: mehtap.tugrak@gop.edu.tr

ABSTRACT

Chalcone molecules are important pharmacophores in medicinal chemistry and have various biological functions, including inhibitory effects on the enzymes carbonic anhydrase (CA) and acetylcholinesterase (AChE). Carbonic anhydrase I and II inhibitors are used in the treatment of disorders such as retinal and cerebral edema (CAI), epilepsy, and glaucoma (CA II). Furthermore, acetylcholinesterase inhibitors, which were originally created to treat Alzheimer's disease, have proven useful for patients suffering from Parkinson's disease-related memory problems, behavioral disorders, and cognitive decline. The drugs on the market have adverse effects. Therefore, new drug candidates are required to address the issues raised. In this study, chalcone compounds were synthesized to investigate their CA and AChE inhibitory effects and their chemical structures were confirmed using NMR. The inhibitory effects of the synthesized compounds on carbonic anhydrase and acetylcholine esterase enzymes were presented for the first time in this study. Carbonic anhydrases and AChE inhibitory effects of 1-21 were investigated using described methodologies. As a result of the studies, it was determined that the compounds were in the inhibition range of 2.65-82.33 µM for hCA I and 2.63-74.89 µM for hCA II, while the IC_{50} values of the reference AZA were 46.75 µM (hCA I) and 38.25 µM (hCA II). Moreover, these compounds inhibited AChE in the range of 15.53-177.46, while the IC_{50} value of the reference drug Tacrin was measured as 25.78 nM. Among the synthesized chalcone derivatives, compound **5** emerged as the most potent inhibitor for hCA I and AChE, while compound **13** was the strongest for hCA II. AutoDock Vina docking results showed that compound **5** had the strongest affinity for hCA I (-8.0 kcal mol^{-1}) and AChE (-7.0 kcal mol^{-1}), while compound **13** was most potent for hCA II (-8.1 kcal mol^{-1}). Key interactions with catalytic residues suggest that halogen and methoxy groups enhance enzyme binding, stability, and hydrogen bonding. These findings suggest that these compounds hold promise as potential drug candidates for CA and AChE related disorders.

Medicinal Chemistry

Research Article

Article History
Received : 26.11.2024
Accepted : 15.02.2025

Keywords
Alzheimer disease
Carbonic anhydrase
Acetylcholinesterase
Molecular docking
Chalcone

Asetilkolinesterazı ve Karbonik Anhidraz Izoenzimlerini Hedef Alan Şalkonların Moleküler Yerleştirme Çalışmaları ve Biyolojik Aktiviteleri

ÖZET

Şalkon molekülleri, medisinal kimyada önemli farmakoforlar olup, karbonik anhidraz (CA) ve asetilkolinesteraz (AChE) enzimleri üzerindeki inhibitör etkiler de dahil çeşitli biyolojik fonksiyonlara sahiptir. Karbonik anhidraz I ve II inhibitörleri, retina ve serebral ödem (CAI), epilepsi ve glokom (CA II) gibi bozuklukların tedavisinde

Medisinal Kimya

Araştırma Makalesi

Makale Tarihçesi
Geliş Tarihi : 26.11.2024

kullanılır. Ayrıca, başlangıçta Alzheimer hastalığını tedavi etmek için oluşturulan asetilkolinesteraz inhibitörlerinin Parkinson hastalığıyla ilişkili hafıza sorunları, davranış bozuklukları ve bilişsel gerileme çeken hastalar için de yararlı olduğu kanıtlanmıştır. Piyasadaki ilaçların olumsuz etkileri bulunmaktadır. Bu nedenle, ortaya çıkan sorunları ele almak için yeni ilaç adaylarına ihtiyaç vardır. Bu çalışmada, CA ve AChE inhibitör etkilerini araştırmak için şalkon bileşikleri sentezlenmiş ve kimyasal yapıları NMR kullanılarak doğrulanmıştır. Bu çalışma ile sentezlenen bileşiklerin karbonik anhidraz ve asetilkolin esteraz enzimleri üzerindeki inhibitör etkileri ilk kez sunulmuştur. Bileşik 1-21'in CA ve AChE inhibitör etkileri açıklanan metodolojiler kullanılarak araştırılmıştır. Yapılan araştırmalar sonucunda bileşiklerin hCA I için 2.65-82.33 µM ve hCA II için 2.63-74.89 µM inhibisyon aralığında olduğu tespit edilirken, referans AZA'nın IC_{50} değerlerinin ise 46.75 µM (hCA I) ve 38.25 µM (hCA II) olduğu görülmüştür. Dahası, bu bileşikler AChE'yi 15.53-177.46 aralığında inhibe ederken, referans ilaç Tacrin'in IC_{50} değeri ise 25.78 nM olarak ölçülmüştür. Sentezlenen şalkon türevleri arasında, bileşik **5** hCA I ve AChE için en etkili inhibitör olarak ortaya çıkarken, bileşik **13** hCA II için en güçlüsüydü. AutoDock Vina ile yapılan molecular docking sonuçlarına göre, bileşik **5** hCA I (-8.0 kcal mol^{-1}) ve AChE (-7.0 kcal mol^{-1}) için en güçlü afiniteyi gösterirken, bileşik **13** hCA II (-8.1 kcal mol^{-1}) için en güçlü inhibitör olarak belirlendi. Kilit katalitik kalıntılarla etkileşimleri, halojen ve metoksi gruplarının enzim bağlanmasını, stabilitesini ve hidrojen bağlarını güçlendirdiğini göstermektedir. Bu bulgular, bu bileşiklerin CA ve AChE ile ilişkili bozukluklar için potansiyel ilaç adayları olarak umut vadettiğini göstermektedir.

Kabul Tarihi : 15.02.2025

Anahtar Kelimeler
Alzheimer Hastalığı
Karbonik Anhidraz
Asetilkolinesteraz
Moleküler Doking
Şalkon

Atıf İçin : Tuğrak-Sakarya, M., Gül, H.İ., Sert, Y., Akıncıoğlu, H., Gülçin, İ., & Gül, M (2025). Asetilkolinesterazı ve Karbonik Anhidraz Izoenzimlerini Hedef Alan Şalkonların Moleküler Yerleştirme Çalışmaları ve Biyolojik Aktiviteleri. *KSÜ Tarım ve Doğa Derg 28* (2), 335-350. DOI: 10.18016/ksutarimdoga.vi.1591728.

To Cite: Tuğrak-Sakarya, M., Gül, H.İ., Sert, Y., Akıncıoğlu, H., Gülçin, İ., & Gül, M (2025). Molecular Docking Studies and Biological Activities of Chalcones Targeting Acetylcholinesterase, and Carbonic Anhydrase Isoenzymes. *KSU J. Agric Nat 28* (2), 335-350. DOI: 10.18016/ksutarimdoga.vi.1591728.

INTRODUCTION

The human lifespan has increased due to advancements in medicine that improve living conditions. Conditions such as dementia are increasingly imposing a significant burden on society due to the rising longevity of individuals. Among the most prevalent illnesses affecting the elderly is dementia. Alzheimer's disease is the most common cause of dementia (AD). (Ferri et al., 2005). Alzheimer's disease is a neurological disease that causes cognitive processes like memory, attention, executive functions, visuospatial skills, and language skills to decrease (Tierney et al., 1996; Petersen et al., 1999; Galvin et al., 2005; Petersen et al., 2006). Currently, research focuses on early detection and effective treatment options. Alzheimer's disease etiology hypotheses include the cholinergic, amyloid, glutamergic, metal, oxidative stress, genetic, and inflammatory hypotheses. The development and activity of the cerebral cortex, cerebral blood flow, sleep cycle, learning, memory, and perception are all significantly influenced by cholinergic transmission. Acetylcholine is a neurotransmitter that causes the smooth muscles in blood vessels to relax and the smooth muscles in the gastrointestinal, urinary, and ocular tracts to contract. The cholinergic hypothesis states that either an increase in the activity of the acetylcholinesterase (AChE) enzyme or a decrease in the brain's generation of acetylcholine, one of the key neurotransmitters, results in a decrease in the amount of acetylcholine. Acetylcholine's carboxylic acid ester group is hydrolyzed by AChE, resulting in the formation of acetic acid and choline. Acetylcholine hydrolyzes in synapses and neuromuscular junctions, preventing nerve transmission. Hence, in the autonomic and somatic nervous systems, AChE is essential for cholinergic neuron transmission. Acetylcholine concentrations in synapses rise as a result of AChE enzyme inhibition, allowing receptors to engage with acetylcholine more intensely and for longer periods of time. Tacrine is an AChE inhibitor first produced for clinical use in 1986. Later, second-generation AChE inhibitors with improved tolerance were developed, including donepezil (1996), rivastigmine (1998), and galantamine (2000) (Knopman et al., 2021; Marucci et al., 2021; Poyraz et al., 2024). In all living organisms, the conversion of carbon dioxide and bicarbonate ions, which are crucial in biochemical processes, to one another is of extreme importance.

Metalloenzymes such as carbonic anhydrase (CAs, EC 4.2.1.1) can utilize certain ions or simple molecules as substrates. Fundamentally, it is understood to catalyze the reaction between bicarbonate and carbon dioxide. To meet the metabolic needs in a shorter amount of time, carbonic anhydrases catalyze this reaction, even though it can occur spontaneously at physiological pH. The Zn^{2+} ion, which is typically tightly bound and interacts with water and histidine molecules in the active site of the enzyme, serves to bind and activate the water molecule, thereby catalyzing the reversible hydration reaction of carbon dioxide to bicarbonate and proton ions through a metal hydroxide nucleophilic mechanism. Humans are known to possess 16 distinct CA isoenzymes (α-hCA) that are members of the α-class. Among them, CA I and CA II are cytosolic isoenzymes. CA I is responsible for acid-base balance and control of respiration. Sweat glands, adipose tissue, the gastrointestinal tract, and the corneal epithelium are among the tissues and cells that contain CA I isoenzyme. One of the isoenzymes that has been examined the most in inhibition studies is CA II. It regulates intraocular pressure by delivering sodium to the eye. This enzyme deficiency is associated with bone resorption, brain calcification, and renal acidity. Furthermore, carbonic anhydrase enzymes play an important role in many physiological and pathological processes. CA inhibitors and CA activators are considered possible treatments for disorders such as edema, glaucoma, obesity, cancer, epilepsy, and osteoporosis due to their role in physiological and pathological processes. Furthermore, CA isoenzymes could be possible targets for Alzheimer's disease (AD) (Supuran et al., 2008; Temperini et al., 2008; Le Duc, et al., 2017).

Chalcones are substances with the chemical formula 1,3-diaryl-2-propen-1-one. They have an α, ß-unsaturated ketone structure. Chalcones are naturally present in many plants due to their simple structure, ease of availability, broad bioactivity spectrum, and tendency to cyclize to produce compounds with therapeutic properties (Ouyang et al., 2021). It has often been taken into consideration when developing new lead compounds with medical potential. Chalcones have a wide range of biological activities, including antibacterial, antifungal, antidiabetic, anti-inflammatory, cytotoxic, and anticancer properties (Mazumder et al., 2024) (Figure 1)

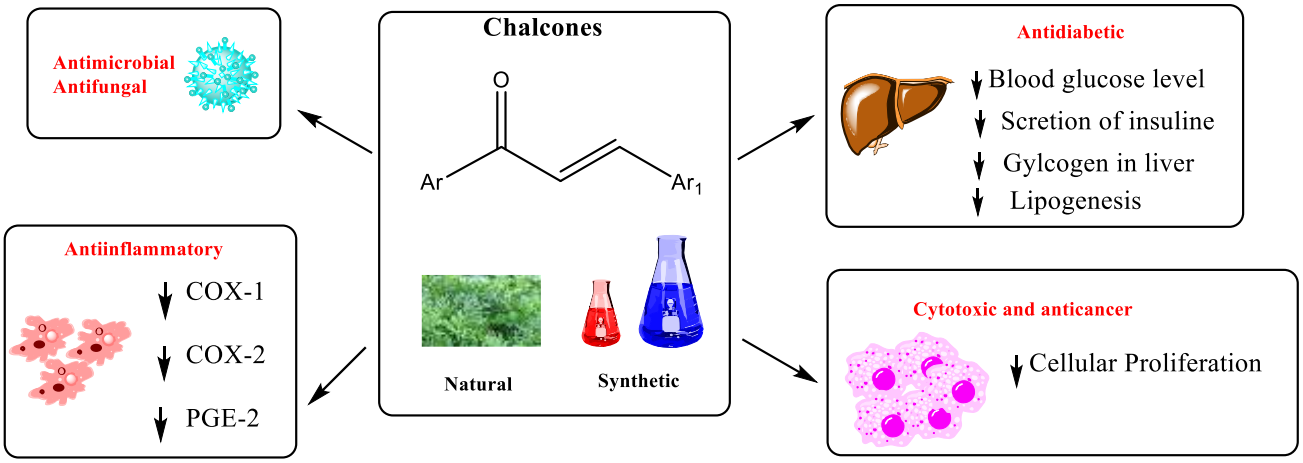


Figure 1 Summarized scheme of some important pharmacological properties of chalcones
Şekil 1 Şalkonların bazı önemli farmakolojik özelliklerinin özet şeması

Due to promising effects obtained according to the works of literature and also as part of our ongoing research survey, in this work, chalcone derivatives (Scheme 1) were investigated in their CAs and AChE inhibition as well as molecular docking was applied.

MATERIAL and METHOD

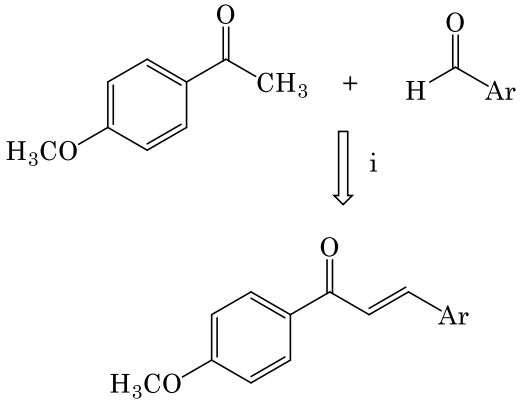
Chemistry

^{1}H NMR (400 MHz) spectra in DMSO-d_6 (Merck) were taken using Varian Mercury Plus spectrometer, Varian Inc., Palo Alto, California, U.S. 9100/IA9100 instrument (Bibby Scientific Limited, Staffordshire, UK) was used to determine melting points. Reactions were monitored by Thin Layer Chromatography (TLC) using silica gel HF254 (Merck Art 5715).

General synthesis procedure of 1-21, Scheme 1

To the mixture of 4-methoxyacetophenone (1 m mol) and a suitable aldehyde (1 m mol) in EtOH (20 ml), NaOH (in aqua 10%, 4 ml) was added. The contents of the flask were stirred at room temperature for 24 hours. The formed

substance is poured into cold water (100 ml) and then HCI (in aqua 10%, w v^{-1}) was added until mixture neutralized. The solid formed was filtered and washed with water. H_2O / Ethanol mixture was used for crystallization (Tugrak et al., 2016; Tugrak et al., 2017; Tugrak et al., 2018) (Scheme 1)



1-21

Ar: 1= Phenyl
2= 4-Methylphenyl
3= 4-Methoxyphenyl
4= 4-Chlorophenyl
5= 4-Bromophenyl
6= 4-Fluorophenyl
7= 2-Chlorophenyl
8= 3-Chlorophenyl
9= 2-Fluorophenyl
10= 3-Fluorophenyl
11= 2,4-Dimethoxyphenyl
12= 2,3-Dimethoxyphenyl
13= 2,3,4-Trimethoxyphenyl
14= 2,4,5-Trimethoxyphenyl
15= 3,4,5-Trimethoxyphenyl
16= 3-Bromophenyl
17= 3-Hydroxy-4-methoxyphenyl
18= Thiophenone-2yl
19= Benzyloxyphenyl
20= Naphthalen-2-yl
21= Benzo[d][1,3]dioxol-5-yl

Reagents: (i) 10% NaOH, EtOH, r.t., 24 h

Scheme 1 Synthesis of the compounds 1-21
Şema 1 Bileşik 1-21'in sentezi

(*E*)-1-(4-Methoxyphenyl)-3-phenylprop-2-en-1-one (1)

Yield: 90%. m. p.: 98-100ºC, Lit m. p.: 99-102ºC (Shinichi et al., 1990). ^{1}H-NMR ($CDCl_3$) δ 8.04 (d, 2H, *J* = 8.8 Hz, Ar-H), 7.80 (d, 1H, *J* = 15.7 Hz, =CH), 7.65-7.63 (m, 2H, Ar-H), 7.54 (d, 1H, *J* = 15.7 Hz, =CH), 7.43-7.37 (m, 3H, Ar-H), 6.98 (d, 2H, *J* = 8.8 Hz, Ar-H), 3.89 (s, 3H, CH_3O)

(*E*)-1-(4-Methoxyphenyl)-3-(*p*-tolyl)-prop-2-en-1-one (2)

Yield: 88%. m. p.: 96-98ºC, Lit m. p.: 95-97ºC (Umesha et al., 2015). ^{1}H-NMR ($CDCl_3$) δ 8.03 (d, 2H, *J* = 8.8 Hz, Ar-H), 7.78 (d, 1H, *J* = 15.6 Hz, =CH), 7.55-7.48 (m, 3H, Ar-H, =CH), 7.25-7.21 (m, 2H, Ar-H), 6.98 (d, 2H, *J* = 8.8 Hz, Ar-H), 3.88 (s, 3H, CH_3O), 3.85 (s, 3H, CH_3O)

(*E*)-1,3-Bis(4-methoxyphenyl)-prop-2-en-1-one (3)

Yield: 91%. m. p.: 96-98ºC, Lit m. p.: 99ºC (Vaidya et al., 2012). ^{1}H-NMR ($CDCl_3$) δ 8.03 (d, 2H, *J* = 8.8 Hz, Ar-H), 7.78 (d, 1H, *J* = 15.5 Hz, =CH), 7.60 (d, 2H, *J* = 8.8 Hz, Ar-H), 7.43 (d, 1H, *J* = 15.5 Hz, =CH), 6.99-6.92 (m, 4H, Ar-H), 3.88 (s, 3H, CH_3O), 3.85 (s, 3H, CH_3O)

(*E*) 1-(4-Methoxyphenyl)-3-(4-chlorophenyl)-prop-2-en-1-one (4)

Yield: 90%. m. p.: 112-114ºC, Lit m. p.: 115ºC (Vaidya et al., 2012). ^{1}H-NMR ($CDCl_3$) δ 8.03 (d, 2H, *J* = 8.7 Hz, Ar-H), 7.74 (d, 1H, *J* = 15.6 Hz, =CH), 7.58-7.49 (m, 3H, Ar-H, =CH), 7.38 (d, 2H, *J* = 8.7 Hz, Ar-H), 6.98 (d, 2H, Ar-H, *J* = 8.8 Hz), 3.89 (s, 3H, CH_3O)

(*E*) 1-(4-Methoxyphenyl)-3-(4-bromophenyl)-prop-2-en-1-one (5)

Yield: 85%. m. p.: 155-156ºC, Lit m. p.: 152-154ºC (Bale et al., 2018). ^{1}H-NMR ($CDCl_3$) δ 8.03 (d, 2H, *J* = 8.8 Hz, Ar-H), 7.72 (d, 1H, *J* =15.6 Hz, =CH), 7.55-7.48 (m, 5H, Ar-H, =CH), 6.98 (d, 2H, *J* = 8.8 Hz, Ar-H), 3.89 (s, 3H, CH_3O)

(*E*) 1-(4-Methoxyphenyl)-3-(4-fluorophenyl)-prop-2-en-1-one (6)

Yield: 80%. m. p.: 113-115°C, Lit m. p.: 115-118°C (Kumar et al., 2012). ^{1}H-NMR ($CDCl_3$) δ 8.04 (d, 2H, *J* = 8.8 Hz, Ar-H), 7.76 (d, 1H, *J* =15.6 Hz, =CH), 7.65-7.61 (m, 2H, Ar-H), 7.47 (d, 1H, *J* = 15.6 Hz, =CH), 7.13-7.08 (m, 2H, Ar-H), 6.94 (d, 2H, *J* = 8.8 Hz, Ar-H), 3.89 (s, 3H, CH_3O)

(*E*) 1-(4-Methoxyphenyl)-3-(2-chlorophenyl)-prop-2-en-1-one (7)

Yield: 81%. m. p.: 117-119°C, Lit m. p.: 118- 120°C (Kazi et al., 2017). ^{1}H-NMR ($CDCl_3$) δ 8.04 (d, 2H, *J* = 8.8 Hz, Ar-H), 7.76 (d, 1H, *J* = 15.6 Hz, =CH), 7.65-7.61 (m, 2H, Ar-H), 7.47 (d, 1H, *J* = 15.6 Hz, =CH), 7.13-7.08 (m, 2H, Ar-H), 6.94 (d, 2H, *J* = 8.8 Hz, Ar-H), 3.89 (s, 3H, CH_3O)

(*E*) 1-(4-Methoxyphenyl)-3-(3-chlorophenyl)-prop-2-en-1-one (8)

Yield: 82%. m. p.: 95-97°C, Lit m. p.: 97-99°C (Abdel-Halim et al., 2013). ^{1}H-NMR ($CDCl_3$) δ 8.04 (d, 2H, *J* = 8.8 Hz, Ar-H), 7.75 (d, 1H, *J* = 15.8 Hz, =CH), 7.62-7.47 (m, 2H, Ar-H, =CH), 7.35 (d, 2H, *J* = 8.9 Hz, Ar-H), 7.08-6.97 (m, 2H, Ar-H), 6.83 (d, 1H, *J* = 8.8 Hz, Ar-H), 3.89 (s, 3H, CH_3O)

(*E*) 1-(4-Methoxyphenyl)-3-(2-fluorophenyl)-prop-2-en-1-one (9)

Yield: 80%. m. p.: 100-102°C, Lit m. p.: 105-106°C (Choi et al., 2015). ^{1}H-NMR ($CDCl_3$) δ 8.04 (d, 2H, *J* = 8.8 Hz, Ar-H), 7.98 (d, 1H, *J* = 15.9 Hz, =CH), 7.66 (d, 1H, *J* = 15.9 Hz, =CH), 7.62-7.35 (m, 1H, Ar-H), 7.21-7.10 (m, 2H, Ar-H), 6.97 (d, 1H, *J* = 8.9 Hz, Ar-H), 3.89 (s, 3H, CH_3O)

(*E*) 1-(4-Methoxyphenyl)-3-(3-fluorophenyl)-prop-2-en-1-one (10)

Yield: 85%. m. p.: 100-102°C, Lit m. p.: 104.5-105.5 °C (Roman et al., 2015). ^{1}H-NMR ($CDCl_3$) δ 8.04 (d, 1H, *J* = 8.8 Hz, Ar-H), 7.77 (d, 2H, *J* = 8.8 Hz, Ar-H), 7.53 (d, 1H, *J* = 15.6 Hz, =CH), 7.40-7.35 (m, 1H, Ar-H), 7.16-7.10 (m, 2H, Ar-H, =CH), 6.98 (d, 1H, *J* = 8.9 Hz, Ar-H), 6.83 (d, 2H, *J* = 8.8 Hz, Ar-H), 3.89 (s, 3H, CH_3O)

(*E*) 1-(4-Methoxyphenyl)-3-(2,4-dimethoxyphenyl)-prop-2-en-1-one (11)

Yield: 91%. m. p.: 85-87°C, Lit m. p.: 82°C (Bandgar et al., 2010). ^{1}H-NMR ($CDCl_3$) δ 8.06-8.01 (m, 3H, Ar-H, =CH), 7.58-7.53 (m, 2H, Ar-H, =CH), 6.97 (d, 2H, *J* = 8.8 Hz, Ar-H), 6.54-6.47 (m, 2H, Ar-H), 3.90 (s, 3H, CH_3O), 3.88 (s, 3H, CH_3O), 3.85 (s, 3H, CH_3O)

(*E*) 1-(4-Methoxyphenyl)-3-(2,3-dimethoxyphenyl)-prop-2-en-1-one (12)

Yield: 86%. m. p.: 100-102°C, Lit m. p.: 99.0–99.5°C (Wu et al., 2011). ^{1}H-NMR ($CDCl_3$) δ 8.10-8.03 (m, 3H, Ar-H, =CH), 7.61 (d, 2H, *J* = 15.8 Hz, =CH), 7.29-7.25 (m, 2H, Ar-H), 7.13-7.06 (m, 1H, Ar-H), 6.98 (d, 2H, *J* = 8.8 Hz, Ar-H), 3.90 (s, 3H, CH_3O), 3.89 (s, 3H, CH_3O), 3.88 (s, 3H, CH_3O)

(*E*)-1-(4-Methoxyphenyl)-3-(2,3,4-trimethoxyphenyl)-prop-2-en-1-one (13)

Yield: 85%. m. p.: 91-92°C, Lit m. p.: 94°C (Russell, 1934). ^{1}H-NMR ($CDCl_3$) δ 8.03 (d, 2H, Ar-H, *J* = 8.8 Hz), 7.97 (d, 1H, *J* = 15.8 Hz, =CH), 7.57 (d, 1H, *J* = 15.8 Hz, =CH), 7.38 (d, 1H, *J* = 8.8 Hz, Ar-H), 6.98 (d, 2H, *J* = 8.8 Hz, Ar-H), 6.72 (d, 1H, *J* = 8.8 Hz, Ar-H), 3.94 (s, 3H, CH_3O), 3.91 (s, 3H, CH_3O), 3.90 (s, 3H, CH_3O), 3.89 (s, 3H, CH_3O)

(*E*)-1-(4-Methoxyphenyl)-3-(2,4,5-trimethoxyphenyl)-prop-2-en-1-one (14)

Yield: 86%. m. p.: 120-122°C, Lit m. p.: 124°C (Roman et al., 2015). ^{1}H-NMR ($CDCl_3$) δ 8.04 (d, 1H, =CH, *J* = 15.5 Hz), 7.93 (d, 2H, *J* = 8.8 Hz, Ar-H),7.48 (d, 1H, *J* = 15.7 Hz, =CH), 6.84 (s, 1H, Ar-H), 6.77 (d, 2H, *J* = 8.8 Hz, Ar-H), 6.21 (s, 1H, Ar-H), 3.80 (s, 6H, 2 x CH_3O), 3.75 (s, 3H, CH_3O), 3.57 (s, 3H, CH_3O)

(*E*)-1-(4-Methoxyphenyl)-3-(3,4,5-trimethoxyphenyl)-prop-2-en-1-one (15)

Yield: 81%. m. p.: 132-134°C, Lit m. p.: 131.1-132.5°C (Kovar et al., 2020). ^{1}H-NMR ($CDCl_3$) δ 8.03 (d, 2H, Ar-H, *J* = 8.8 Hz), 7.71 (d, 1H, *J* = 15.6 Hz, =CH), 7.42 (d, 1H, *J* = 15.6 Hz, =CH), 6.98 (d, 2H, *J* = 8.8 Hz, Ar-H), 6.86 (s, 2H, Ar-H), 3.92 (s, 6H, 2xCH_3O), 3.90 (s, 3H, CH_3O), 3.89 (s, 3H, CH_3O)

(*E*) 1-(4-Methoxyphenyl)-3-(3-bromophenyl)-prop-2-en-1-one (16)

Yield: 75%. m. p.: 121-123°C, Lit m. p.: 126°C (Patil et al., 2007). ^{1}H-NMR ($CDCl_3$) δ 7.72 (d, 2H, *J* = 8.8 Hz, Ar-H), 7.32-7.26 (m, 1H, Ar-H, =CH), 7.18-7.11 (m, 4H, Ar-H, =CH), 6.98 (d, 1H, *J* = 8.9 Hz, Ar-H), 6.83 (d, 2H, *J* = 8.8 Hz, Ar-H), 3.89 (s, 3H, CH_3O)

(*E*) 1-(4-Methoxyphenyl)-3-(3-hydroxy-4-methoxyphenyl)-prop-2-en-1-one (17)

Yield: 70%. m. p.: 148-150ºC, Lit m. p.: 150-152ºC (Raghavan et al., 2015). ^{1}H-NMR (DMSO-d_6) δ 9.12 (bs, OH), 8.13 (d, 2H, J= 8.8 Hz, Ar-H), 7.69 (d, 1H, J= 15.4 Hz, =CH), 7.58 (d, 1H, J= 15.4 Hz, =CH), 7.32-7.27 (m, 2H, Ar-H), 7.07 (d, 2H, J= 8.8 Hz, Ar-H) 6.98 (d, 1H, J= 8.3 Hz, Ar-H), 3.86 (s, 3H, CH_3O), 3.83 (s, 3H, CH_3O)

(*E*)-1-(4-Methoxyphenyl)-3-(thiophen-2-yl)-prop-2-en-1-one (18)

Yield: 72%. m. p.: 103-105ºC, Lit m. p.: 106-107ºC (Shibata et al., 1991). ^{1}H-NMR ($CDCl_3$) δ 8.02 (d, 2H, J= 8.8 Hz, Ar-H), 7.93 (d, 1H, J= 15.3 Hz, =CH), 7.41-7.33 (m, 3H, Ar-H, =CH), 7.09-7.07 (m, 1H, Ar-H), 6.98 (d, 2H, J= 8.8 Hz, Ar-H), 3.89 (s, 3H, CH_3O)

(*E*) 1-(4-Methoxyphenyl)-3-(4-(benzyloxy)phenyl)-prop-2-en-1-one (19)

Yield: 76%. m. p.: 132-133ºC, Lit m. p.: 135-137ºC (Bale et al., 2018). ^{1}H-NMR ($CDCl_3$) δ 8.03 (d, 2H, J= 8.8 Hz, Ar-H), 7.84 (d, 1H, J= 8.8 Hz, Ar-H), 7.77 (d, 1H, J= 15.3 Hz, =CH), 7.59 (d, 2H, J= 8.8 Hz, Ar-H), 7.45-7.34 (m, 6H, Ar-H, =CH), 7.09-6.96 (m, 3H, Ar-H), 5.11 (s, 2H, OCH_2), 3.88 (s, 3H, CH_3O)

(*E*)-1-(4-Methoxyphenyl)-3-(naphthalen-2-yl)-prop-2-en-1-one (20)

Yield: 84%. m. p.: 151-152ºC, Lit m. p.: 155ºC (Mai et al., 2014). ^{1}H-NMR ($CDCl_3$) δ 8.65 (d, 1H, J= 15.4 Hz, =CH), 8.27 (d, 1H, J= 8.0 Hz, Ar-H), 8.09 (d, 2H, J= 8.9 Hz, Ar-H), 7.93-7.88 (m, 3H, Ar-H), 7.65-7.50 (m, 4H, Ar-H, =CH), 6.98 (d, 2H, J= 8.9 Hz, Ar-H), 3.89 (s, 3H, CH_3O)

(*E*) 1-(4-Methoxyphenyl)-3-(benzo[*d*][1,3]dioxol-5-yl)-prop-2-en-1-one (21)

Yield: 78%. m. p.: 132-133ºC, Lit m. p.: 134-135ºC (Schwartz et al., 1977). ^{1}H-NMR ($CDCl_3$) δ 8.02 (d, 2H, J= 8.8 Hz, Ar-H), 7.72 (d, 1H, J= 15.5 Hz, =CH), 7.38 (d, 1H, J= 15.5 Hz, =CH), 7.17-7.10 (m, 2H, Ar-H), 6.97 (d, 2H, J= 8.8 Hz, Ar-H), 6.84 (d, 1H, J= 8.0 Hz, Ar-H), 6.02 (s, 2H, OCH_2O), 3.88 (s, 3H, CH_3O)

PHARMACOLOGICAL/BIOLOGICAL ASSAYS

AChE inhibition study

The effects of compounds on AChE enzyme were investigated. Two substrates which are 5,5-dithiobis(2-nitrobenzoic acid) (DTNB) and acetylcholiniodate (AChI) were used in the inhibition tests. In addition, Tris / HCl (100 ml, 1M, pH = 8) buffer was used in this method for AChE enzyme. The final volume was completed to 100 µL and changes in the absorption were followed at 412 nm. The IC_{50} values of the compounds were calculated via activity (%) versus compounds concentration plots (Tugrak et al., 2021c, Yurt et al., 2024; El-Sayed et al., 2019).

hCA Inhibition studies

Human CA isoforms (hCA I and hCA II) were isolated using the sepharose - 4B-L- tyrosine sulfanilamide affinity segregation process, as previously reported. Protein concentrations were measured using the Bradford method at 595 nm. The compounds' inhibitory effects were studied by measuring esterase activity in accordance with Verpoorte et al., as described in prior investigations. The hCA activity was evaluated by monitoring the conversion of the p-nitrophenyl acetate substrate to p-nitrophenolate at 348 nm using a spectrophotometer (UV-VIS Spectrophotometer, UV mini-1240, Shimadzu Corporation). Acetazolamide (AZA) was utilized as the control medication. (Kocyigit et al., 2017; Bradford, 1976; Verpoorte et al., 1967; Guney et al., 2014; Tugrak et al., 2020; Tugrak et al., 2021a; Tugrak et al., 2021b).

Computation Method

In this study, *in silico* docking analyses were performed using the AutoDock Vina (Trott et & Olson, 2010) program. The molecular structures (**1-21**) were optimized in their ground state and gas phase employing Density Functional Theory (DFT) with the B3LYP functional and the 6-311++G(d,p) basis set, utilizing the Gaussian 09W software package (Frisch et al., 2009). Three-dimensional representations of the optimized structures were generated using the GaussView program (Dennington et al., 2009), without imposing symmetry constraints.

RESULTS and DISCUSSION

Chemistry

Chalcones **1-21** were synthesized by reacting suitable aldehyde with 4-methoxyacetophenone under alkaline conditions at room temperature *via* Claisen-Schmidt Condensation (Scheme 1 and Figure 2). The progress of the

reaction was monitored by TLC. After the reaction, the mixture was cooled in ice water and acidified with 10% HCl until pH = 7. The crystals were obtained by crystallization in an ethanol-water mixture. Confirmation of compound structures was done via melting points and ^{1}H NMR spectra. Experimental part details the chalcones' (1-21) characterization by ^{1}H NMR. Chalcones are open chain flavonoids. Chemically they consist of α, ß-unsaturated carbonyl system, and two aromatic rings. They are available in both cis (*Z*) and trans (*E*) forms. In this work, the compounds were seen as E isomer on the basis of coupling constants. Olefinic carbon-carbon bond of each chalcone was established by their large trans coupling constants (*J*) in the range of 15-16 Hz in the ^{1}H NMR spectra.

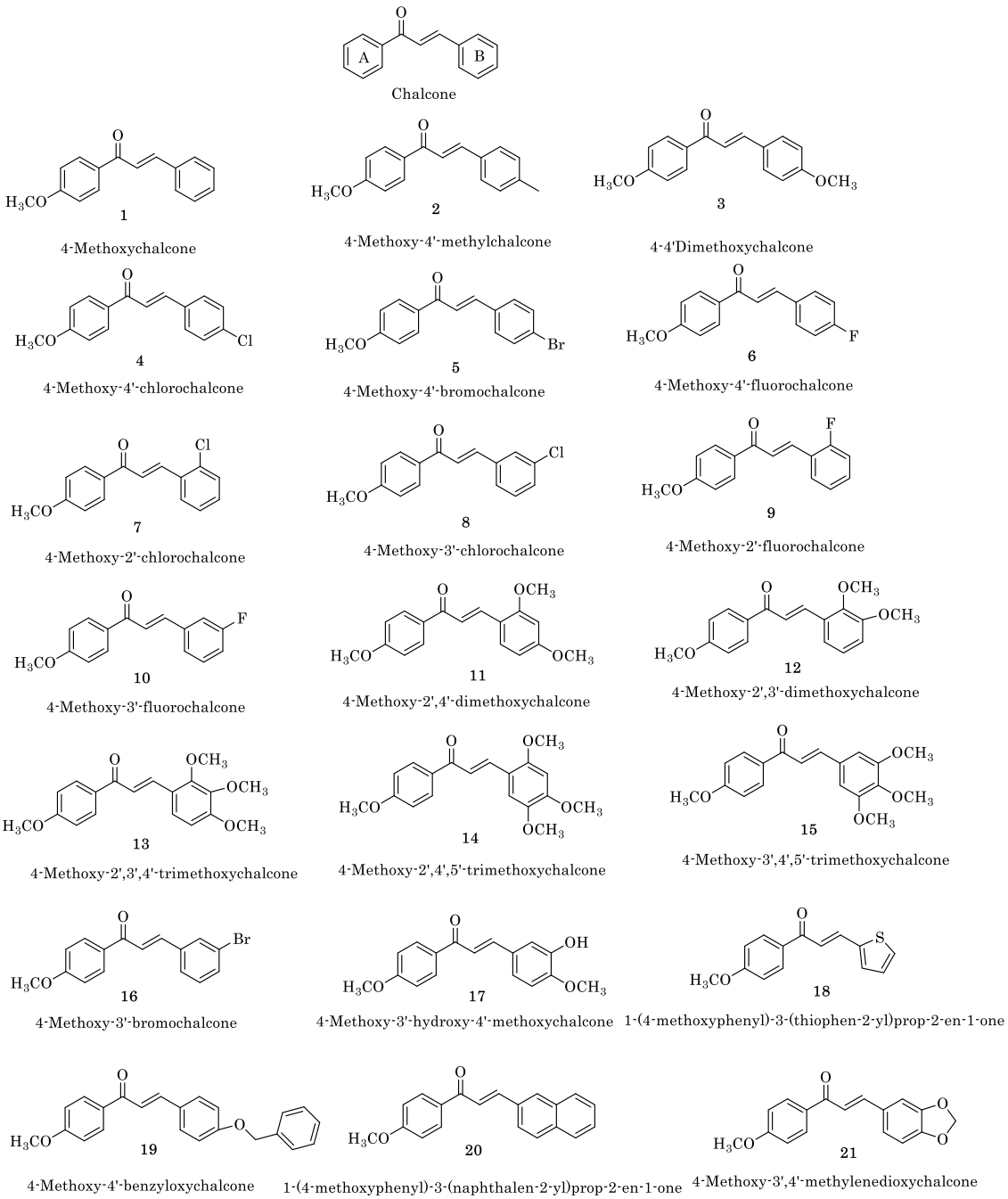


Figure 2 Chemical structure of chalcones used in this study.
Şekil 2 Bu çalışmada kullanılan şalkonların kimyasal yapısı

Bioactivity results

The inhibitory effects of 4-methoxychalcone derivatives on hCA I, hCA II, and AChE were investigated in this study. The IC_{50} values of the chalcones were calculated using Activity (%)-[Chalcone]. The inhibitory data are compiled in Table 1, alongside those pertaining to acetazolamide (AZA), utilized as a standard inhibitor for both hCA isoenzymes. To assess the impact of chalcone derivatives (**1-21**) on the specified metabolic enzymes, the

subsequent results have been presented:

(i) Physiologically significant hCA I is predominantly present in erythrocytes and is also expressed in normal colonic mucosa (Mikus et al., 2018). Regarding CA I, all chalcone derivatives (**1-21**) exhibited IC_{50} values in the low nanomolar range, specifically between 2.65 µM and 82.33 µM. Among the synthesized chalcone derivatives (**1-21**), chalcone **5**, with a bromo group in the meta position, exhibited the highest inhibition (IC_{50}: 2.65 µM), followed by chalcone **4** (IC_{50}: 3.08 µM) in comparison to AZA (Table 1). AZA, serving as a positive control and utilized as a therapeutic medication, exhibited a IC_{50} value of 46.75 µM. The analysis of inhibitory results indicated that halogenated compounds exhibited greater inhibition. All chalcones exhibited superior hCA I inhibition compared to AZA, with the exception of compounds **17** (IC_{50}: 82.33), **18** (IC_{50}: 77.91), **19** (IC_{50}: 56.62), and **21** (IC_{50}: 48.43).

(ii) The chalcones **1-21** demonstrated IC_{50} values ranging from 2.63 to 74.89 µM against the predominant cytosolic hCA II isoform (Table 1). Many chalcones were found to have strong inhibitory effects on hCA II isoenzyme. AZA also revealed an IC_{50} of 38.25 µM against the hCA II isoenzyme. Based on the IC_{50} values, compound **13** exhibited a potency 14.5 times greater than AZA against hCA II. Additionally, compound **20** may be regarded as the second most powerful drug, exhibiting an IC_{50} value of 6.32 nM against hCA II, as indicated in Table 1. The IC_{50} data indicated that lead compound **13** inhibited hCA II with 7.2 times more selectivity than hCA I.

Table 1 The enzyme inhibition parameters of the compounds 1-21 against carbonic anhydrase isoenzyme I and II (CA I, II), acetylcholinesterase (AChE) enzyme

Çizelge 1 Bileşik 1-21'in karbonik anhidraz izoenzim I ve II (CA I, II), asetilkolinesteraz (AChE) enzimine karşı enzim inhibisyon parametreleri

Compound No	CA-I (IC_{50}, µM)	r^2	CA-II (IC_{50}, µM)	r^2	AChE (IC_{50}, µM)	r^2
1	24.0	0.9522	48.15	0.8423	177.46	0.871
2	28.73	0.94	48.02	0.872	53.72	0.8901
3	6.90	0.9377	64.23	0.8518	18.0	0.9301
4	3.08	0.8704	30.83	0.9899	52.46	0.9158
5	2.65	0.9614	21.98	0.865	15.53	0.9932
6	11.74	0.9925	29.61	0.8914	80.97	0.9144
7	15.10	0.9927	30.97	0.8545	53.47	0.9508
8	12.0	0.9502	26.79	0.8832	70.41	0.9752
9	33.13	0.8865	16.62	0.861	89.95	0.9504
10	9.44	0.8894	48.02	0.8933	81.18	0.8936
11	18.67	0.874	9.37	0.979	143.0	0.8584
12	21.18	0.9164	22.11	0.9577	96.62	0.9829
13	18.99	0.8133	2.63	0.974	135.19	0.8858
14	32.69	0.916	52.69	0.8989	160.27	0.8506
15	36.0	0.9556	51.41	0.8415	143.98	0.8804
16	31.85	0.8948	43.69	0.9825	62.88	0.8891
17	82.33	0.9135	74.89	0.9163	61.44	0.9863
18	77.91	0.8144	39.58	0.9945	94.21	0.8325
19	56.62	0.8451	9.38	0.9283	98.73	0.9505
20	24.63	0.86	6.32	0.8576	69.94	0.9759
21	48.43	0.8998	16.58	0.9219	94.81	0.967
AZA	46.75	0.955	38.25	0.833	-	-
Tacrine	-	-	-	-	25.78	0.989

(iii) The AChE inhibitory effects of the synthesized compounds were assessed using Ellman's technique, consistent with prior research employing the reference drug tacrine (Ellman et al., 1961). Tacrine, the first AChE inhibitor used in clinical trials, was withdrawn from the market due to hepatotoxicity. Even while drugs like donepezil, galantamine, and rivastigmine are available, their efficacy remains poor. As a result, research into new anti-AD drug possibilities remains popular. Table 1 indicates that the chemicals evaluated exhibited IC_{50} values ranging from 15.53 to 177.46 µM against the AChE enzyme. Compounds **3** and **5** exhibited significant inhibitory effects with low IC_{50} values of 18.0 µM and 15.53 µM, respectively. Considering the IC_{50} value, compound 5 was deemed the most effective acetylcholinesterase inhibitor in the series.

***TAC: nm**

Molecular Docking

Molecular docking is a computational technique used to predict the interaction between a ligand and a receptor, often within the context of drug discovery. This approach is frequently used in drug design and discovery because it helps scientists find possible therapeutic candidates by modeling molecular interactions and forecasting how well a drug might attach to its target. In order to further the development of therapeutic drugs, scientists can optimize the design of novel compounds with enhanced efficacy, selectivity, and decreased adverse effects by examining these interactions (Karagac et al., 2024; Demir Y, 2020). It involves simulating how a small molecule, such as a drug candidate, fits into the active site of a target protein, evaluating binding affinity and potential interactions. By predicting how well the molecule binds and interacts with the protein, docking helps in identifying promising drug candidates before experimental testing (Erdogan et al., 2024; Demir et al., 2024). The process typically employs algorithms to explore the conformational space of both the ligand and the receptor, aiming to identify the most energetically favorable binding pose. Scoring functions are integral to docking, quantifying the strength of interactions such as hydrogen bonding, hydrophobic effects, and electrostatic forces. Advances in molecular docking have incorporated machine learning to improve accuracy, though challenges such as receptor flexibility and water-mediated interactions remain significant. This method continues to play a crucial role in streamlining the drug discovery process, reducing the cost and time associated with experimental screening (Taylor et al., 2002; Ferreira et al., 2015; Meng et al., 2011). At this stage of the study, the molecular docking or interactions of **1-21** molecules with hCA I (PDB: 2CAB), hCA II (PDB: 5AML), and AChE (PDB: 1EVE) targets were examined with the help of Autodock Vina (Trott et & Olson, 2010), a free program that allows its users. First of all, molecules **1-21** were quantitatively optimized using DFT/B3LYP theory/functional and 6-311++G (d,p) basis set with the help of Gaussian 09W package program (Frisch et al., 2009) and Gauss View 5.0 interface (Dennington et al., 2009) programs. Based on both experimental and theoretical results, the three-dimensional optimization structures of only compounds **5** and **13** were given in Figure 3. The sum of electronic and zero-point energies for these compounds were calculated as -3325.54720857 and -1106.02428896 a.u, respectively.

The ligands (**1-21**) were subsequently converted into PDB and PDBQT formats, with all ligand-related processes conducted using the Discovery Studio Visualizer 4.0 (DSV 4.0) software (Scientific Software). Based on experimental protocols and relevant literature, the target proteins selected for this study were hCA I (PDB ID: 2CAB) (Kannan et al., 1984; Mahmudov et al., 2022), hCA II (PDB ID: 5AML) (Mahmudov et al., 2022; Ivanova et al., 2015), and AChE (PDB ID: 1EVE) (Mahmudov et al., 2022; Kryger et al., 1999). The three-dimensional PDB structures of these receptors were obtained from the RCSB Protein Data Bank (PDB) (Protein Data Bank). Similarly, heteroatoms present in the three target proteins were removed using Discovery Studio Visualizer 4.0 (DSV 4.0) (Scientific Software). Polar hydrogen atoms and their corresponding charges were subsequently added, and the processed data were saved again in PDB and PDBQT formats. To enhance the precision of the docking analysis, the active sites and key residues of the target proteins were identified as follows: HIS119, HIS96, and HIS94 for hCA I (PDB ID: 2CAB); THR200, THR199, LEU198, PHE131, VAL121, HIS119, HIS96, HIS94, GLN92, ASN67, and ASN62 for hCA II (PDB ID: 5AML); and HIS440, PHE330, GLU327, TRP279, SER200, and TRP84 for AChE (PDB ID: 1EVE) (Mert et al., 2025). To incorporate these active zones, the following grid parameters were developed: 40 x 40 x 40 $Å^3$ x, y, z dimensions, 0.375 Å space and 39.041, - 10.534, 10.394 x, y, z centers for hCA I / PDB: 2CAB; 32 x 40 x 32 $Å^3$ x, y, z dimensions, 0.375 Å space and -5.915, 5.359, 16.391 x, y, z centers for hCA II / PDB: 5AML; 44 x 44 x 38 $Å^3$ x, y, z dimensions, 0.375 Å space and -0.39, 63.448, 67.71 x, y, z centers for AchE / PDB: 1EVE (Mert et al., 2025). Among the tested ligands, compound **5** demonstrated the strongest binding affinity to hCA I (-8.0 kcal mol^{-1}) and AChE (-7.0 kcal mol^{-1}), while compound **13** exhibited the highest binding affinity to hCA II (-8.1 kcal mol^{-1}). The binding modes and interactions of these compounds were visualized to elucidate key stabilizing interactions such as hydrogen bonds and hydrophobic effects. Detailed molecular docking results for all compounds are presented in Table 2, highlighting the varying affinities across the three targets. The findings reveal that the compounds exhibit diverse binding profiles, with compounds **5** and **13** emerging as potent inhibitors, hence the interactions between these molecules and their respective proteins were given in Figures. 4-6. Figure 4 illustrates the docking pose and molecular interactions of ligand 5 with human carbonic anhydrase isozyme I (hCA I). Panel (a) provides a three-dimensional visualization of ligand **5** within the active site of hCA I, highlighting its strategic positioning to interact with critical residues. Panel (b) offers a detailed two-dimensional interaction map, showcasing the specific types of interactions. Ligand **5** forms hydrogen bonds with GLN92 and HIS119, which play a pivotal role in stabilizing the ligand-protein complex.

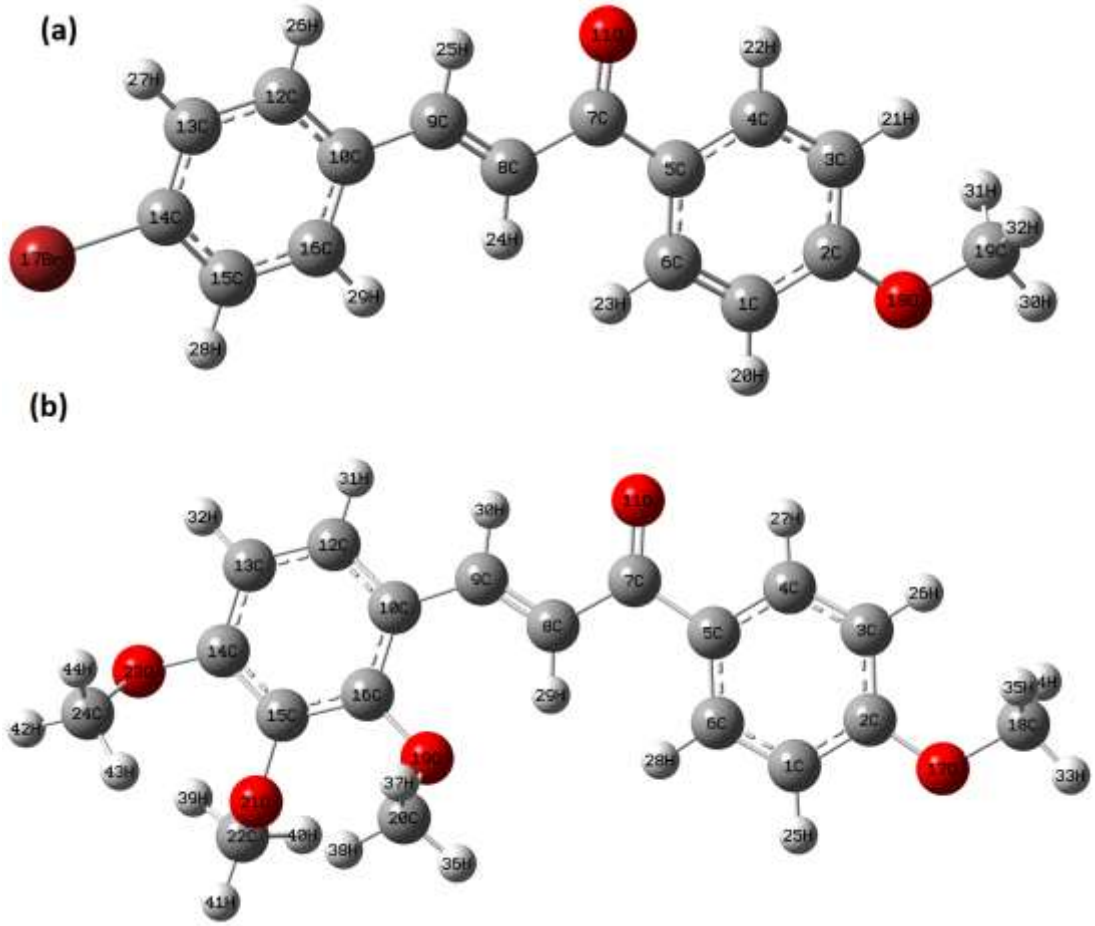


Figure 3 The optimized structures of 5 (a) and 13 (b) molecules.
Şekil 3 5 (a) ve 13 (b) moleküllerinin optimize edilmiş yapıları.

Additionally, Pi - Pi stacking interactions with HIS94 and HIS200, and alkyl interactions with LEU198, contribute to the compound's binding stability. The close proximity of ligand **5** to the catalytic zinc ion suggests potential competitive inhibition, rendering it a potent inhibitor of hCA I activity. This comprehensive interaction profile underscores ligand **5**'s high binding affinity (-8.0 kcal mol^{-1}) as reported in the docking analysis, confirming its potential as a selective inhibitor. Figure 5 demonstrates the binding interaction of ligand **13** within the active site of hCA II. In panel (a), the three-dimensional docking visualization highlights the ligand's orientation relative to the catalytic pocket. Panel (b) elaborates on the molecular interactions, showing critical hydrogen bonds with residues such as GLN92 and THR200. These interactions are complemented by carbon hydrogen bonds with HIS94 and van der Waals interactions with VAL121 and LEU198, ensuring ligand stability within the active site. π-donor hydrogen bonding and π-Sigma interactions with THR200 further enhance binding specificity. The reported binding affinity of ligand **13** (-8.1 kcal mol^{-1}) aligns with these interactions, confirming its superior inhibitory potential against hCAII compared to other compounds in the study. The high specificity and stability of ligand **13** make it a promising candidate for targeting hCA II-related pathologies. Figure 6 presents the molecular docking results of ligand **5** with acetylcholinesterase (AChE). Panel (a) shows the ligand's three-dimensional positioning within the enzyme's active site, while panel (b) provides a detailed interaction map. Ligand **5** forms π-π stacking interactions with TRP84 and PHE330, which are critical for substrate recognition and inhibition. Additional hydrogen bonds with HIS440 and van der Waals interactions with GLU199 and ILE444 further stabilize the ligand within the catalytic pocket. The compound also engages in alkyl interactions with TYR334, contributing to its binding affinity. The docking score of ligands **5** (-7.0 kcal mol^{-1}) reflects these diverse and strong interactions, demonstrating its potential as an effective AChE inhibitor. These results support the hypothesis that ligand **5** may act as a competitive inhibitor, interfering with substrate binding and enzymatic activity.

Table 2 Molecular docking scores of **1-21** compounds.
*Çizelge 2 **1-21** bileşiklerin moleküler yerleştirme puanları.*

Compounds	**hCA I / PDB: 2CAB + ligands** Affinity (kcal mol^{-1})	**hCA II / PDB: 5AML + ligands** Affinity (kcal mol^{-1})	**AChE / PDB: 1EVE + ligands** Affinity (kcal mol^{-1})
1	-6.8	-6.6	-6.9
2	-7.0	-6.8	-6.7
3	-6.7	-6.8	-6.6
4	-6.4	-6.5	-6.7
	-8.0	-6.6	-7.0
5	Ki =1.36759 µM H. B = 1		Ki =7.39542 µM H. B =0
6	-7.3	-6.5	-6.5
7	-6.7	-6.8	-6.5
8	-6.9	-6.9	-6.4
9	-7.0	-6.8	-5.9
10	-6.8	-7.0	-6.8
11	-6.2	-6.8	-6.9
12	-7.0	-7.3	-6.9
	-6.6	-8.1	-6.9
13		Ki =1.1552 µM H. B = 1	
14	-5.9	-6.7	-6.0
15	-6.1	-6.1	-6.4
16	-7.0	-7.1	-6.9
17	-6.4	-6.5	-6.3
18	-6.1	-6.4	-5.8
19	-6.7	-7.4	-6.9
20	-7.9	-7.9	-6.8
21	-7.9	-7.7	-6.9

Ki: Inhibition constant
H. B: Hydrogen Bonding

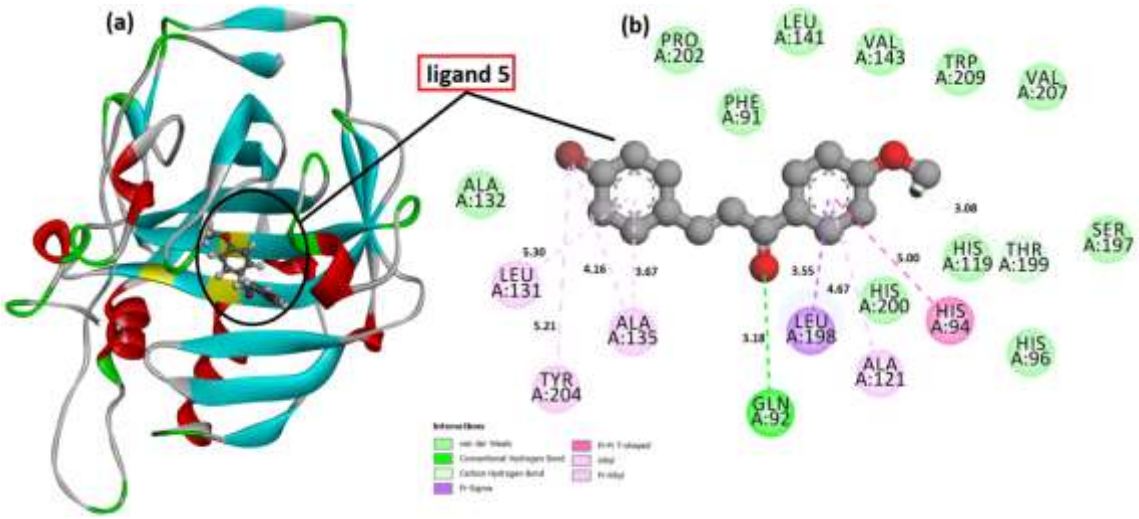


Figure 4 The localization of the molecule to the active site of the protein 2CAB (a) and 2D (b) molecular docking results for compound **5** and PDB: 2CAB.
*Şekil 4 Molekülün protein 2CAB'nin aktif bölgesine lokalizasyonu (a) ve 2D (b) bileşik **5** ve PDB:2CAB için moleküler yerleştirme sonuçları*

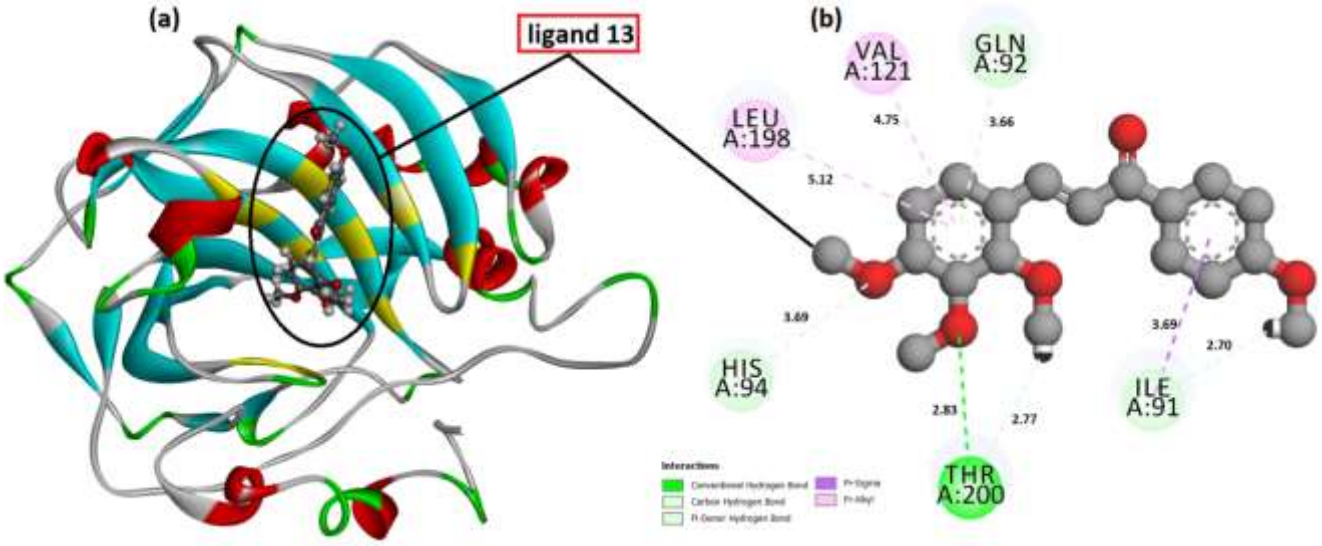


Figure 5 The localization of the molecule to the active site of the protein 5AML (a) and 2D (b) molecular docking results for compound 13 and PDB: 5AML.

Şekil 5 Molekülün protein 5AML'nin aktif bölgesine lokalizasyonu (a) ve 2D (b) bileşik 13 ve PDB: 5AML için moleküler yerleştirme sonuçları

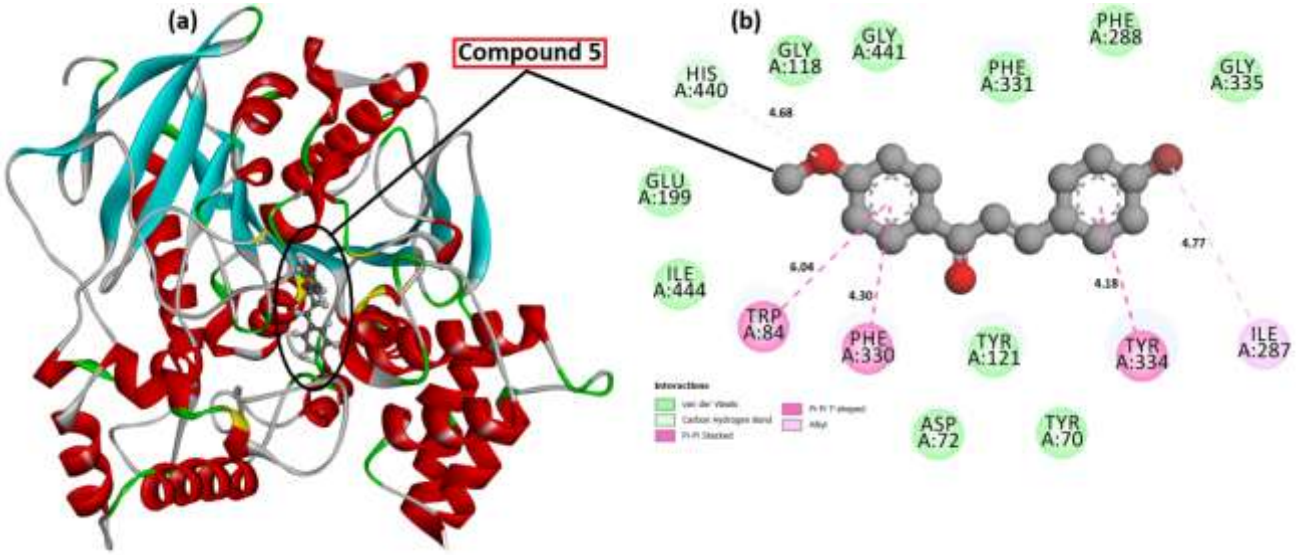


Figure 6 The localization of the molecule to the active site of the protein 1EVE (a) and 2D (b) molecular docking results for compound 5 and PDB: 1EVE.

Şekil 6 Molekülün protein 1EVE'nin aktif bölgesine lokalizasyonu (a) ve 2D (b), bileşik 5 ve PDB: 1EVE için moleküler yerleştirme sonuçları

CONCLUSION

In conclusion, chalcone derivatives were successfully produced with high yields and they were evaluated for their inhibitory potentials on the hCA I, hCA II, and AChE enzymes. The computational evaluation of current enzyme inhibitors and molecular docking analysis was also performed. According to the IC_{50} values, compound **5** and compound **13** were 17.6 and 14.5 times more potent than the reference acetazolamide against hCA I and hCA II, respectively. Compound **5** significantly inhibited AChE at micromolar doses. The inhibitory potential of the newly synthesized compounds (**1-21**) against hCA I (PDB: 2CAB), hCA II (PDB: 5AML), and AChE (PDB: 1EVE) was

evaluated through *in silico* molecular docking simulations utilizing the AutoDock Vina platform. Compound **5** showed the highest docking score for hCA I (-8.0 kcal mol^{-1}) and AChE (-7.0 kcal mol^{-1}), indicating a favorable interaction with key catalytic residues such as HIS119, HIS94, and HIS96 in hCA I, and TRP84 and PHE330 in AChE. Compound **13** displayed the best docking score for hCA II (-8.1 kcal mol^{-1}), interacting with critical residues GLN92, THR200, and HIS94, suggesting a strong stabilizing effect within the enzyme's active site. These results demonstrate that the halogen and methoxy substituents in compounds **5** and **13** likely contribute to their enhanced enzyme-ligand interactions, hydrogen bonding potential, and overall stability within the binding pocket. Additionally, the agreement between computational predictions and experimental IC50 values highlights the reliability of molecular docking as a predictive tool. A strong concordance between the computational predictions and experimental data was observed, underscoring the reliability of the applied approach. These findings indicate that these compounds, alongside existing market agents, hold significant promise as inhibitors targeting AChE, hCA I, and hCA II proteins. Overall, prospective investigations have identified possible compounds **5** and **13** for CAs and compound **5** for AChE. Compounds **5** and **13** can be considered as remarkable candidates for further studies. Inother words, given their potent inhibition profiles, compounds **5** and **13** are strong candidates for further optimization and preclinical evaluation in the development of novel inhibitors targeting carbonic anhydrase and acetylcholinesterase-related disorders. At the same time, compounds synthesized by molecular modifications can be supported by *in vivo* studies in future studies.

ACKNOWLEDGMENTS

The authors especially thanks to Prof. Dr. Fatih UCUN for his helpful contribution for Gaussian calculations, Dr. Barıs Anıl for contributions and TUBITAK for financial support (Project Number: 117S939)

Contribution Rate Statement Summary of Researchers

Mehtap Tugrak Sakarya, investigation, methodology, writing – original draft, review & editing, Halise Inci Gul and Mustafa Gul, review & editing, supervision, Yusuf Sert, carried out the molecular docking studies, Hulya Akıncıoglu and Ilhami Gulcin were conducted biological activity tests. All authors have read and agreed to the published version of the manuscript.

Conflict of Interest

The author declared no potential conflicts of interest with respect to the research, authorship, and publication of this article.

My article to be published does not require ethics committee approval and/or legal/special permission.

REFERENCES

Abdel-Halim, M., Keeton, A. B., Gurpinar, E., Gary, B. D., Vogel, S. M., Engel, M., & Abadi, A. H. (2013). Trisubstituted and tetrasubstituted pyrazolines as a novel class of cell-growth inhibitors in tumor cells with wild type p53. *Bioorganic & Medicinal Chemistry, 21*(23), 7343-7356.

Bale, A. T., Khan, K. M., Salar, U., Chigurupati, S., Fasina, T., Ali, F., & Perveen, S. (2018). Chalcones and -chalcones: As potential α-amylase inhibitors; synthesis, screening, and molecular modelling studies. *Bioorganic Chemistry, 79*, 179-189.

Bandgar, B. P., Gawande, S. S., Bodade, R. G., Totre, J. V., & Khobragade, C. N. (2010). Synthesis and biological evaluation of simple methoxylated chalcones as anticancer, anti-inflammatory and antioxidant agents. *Bioorganic & Medicinal Chemistry, 18*(3), 1364-1370.

Bradford, M. M. (1976). A rapid and sensitive method for the quantitation of microgram quantities of protein utilizing the principle of protein-dye binding. *Analytical Biochemistry,* 72, 248-254.

Choi, J. W., Jang, B. K., Cho, N. C., Park, J. H., Yeon, S. K., Ju, E. J., & Park, K. D. (2015). Synthesis of a series of unsaturated ketone derivatives as selective and reversible monoamine oxidase inhibitors. *Bioorganic & Medicinal Chemistry, 23*(19), 6486-6496.

Demir, Y. (2020). Naphthoquinones, benzoquinones, and anthraquinones: Molecular docking, ADME and inhibition studies on human serum paraoxonase-1 associated with cardiovascular diseases. *Drug Development Research,* 81(5), 628-636

Demir, Y., Ozturk N., Isıyel, M., Ceylan, H. (2024). Effects of Carnosic and Usnic Acid on Pentose Phosphate Pathway Enzymes: An Experimental and Molecular Docking Study. *ChemistrySelect*, 9, e202401067

Dennington, R., Keith, T., Millam, J. (2009). GaussView, version 5, Semichem Inc.: Shawnee Mission, KS.

Ellman, G. L., Courtney, K. D., Andres Jr, V., & Featherstone, R. M. (1961). A new and rapid colorimetric determination of acetylcholinesterase activity. *Biochem. Pharma, 7*(2), 88-90.

El-Sayed, N. A., Farag, A. E., Ezzat, M. A. F., Akincioglu, H., Gulcin, I., Abou-Seri, S. M. (2019). Design, synthesis, in vitro and in vivo evaluation of novel pyrrolizine-based compounds with potential activity as cholinesterase inhibitors and anti-Alzheimer's agents. *Bioorg. Chem*, 93, 10.3312

Erdogan, M., Onder, A., Demir Y., Onder, F. C. (2024). Novel Dibenzoazepine-Substituted Triazole Hybrids as Cholinesterase and Carbonic Anhydrase Inhibitors and Anticancer Agents: Synthesis, Characterization, Biological Evaluation, and In Silico Studies. *ACS Omega,* 9, 46860−46878.

Ferreira, L. G., Dos Santos, R. N., Oliva, G., Andricopulo, A. D. (2015). Molecular docking and structure-based drug design strategies, *Molecules*, 20(7), 13384-13421.

Ferri, C. P., Prince, M., Brayne, C., Brodaty, H., Fratiglioni, L., Ganguli, M., & Intl, A. D. (2005). Global prevalence of dementia: a Delphi consensus study. *Lancet, 366*(9503), 2112-2117.

Frisch, M.J., Trucks, G., Schlegel, H., Scuseria, G., Robb, M., Cheeseman, J., Scalmani, G., Barone, V., Mennucci, B., Petersson, G. (2009). Gaussian 09, Revision D. 01, Gaussian, Inc.: Wallingford, CT.

Galvin, J. E., Powlishta, K. K., Wilkins, K., McKeel, D. W., Xiong, C. J., Grant, E., & Morris, J. C. (2005). Predictors of-preclinical Alzheimer disease and dementia - A clinicopathologic study. *Archives of Neurology, 62*(5), 758-765.

Guney, M., Coskun, A., Topal, F., Dastan, A., Gulcin, I., Supuran, C.T. (2014). Oxidation of cyanobenzocycloheptatrienes: Synthesis, photooxygenation reaction and carbonic anhydrase isoenzymes inhibition properties of some new benzotropone derivatives. *Bioorganic & Medicinal Chemistry,* 22(13), 3537-3543.

Ivanova, J., Leitans, J., Tanc, M., Kazaks, A., Zalubovskis, R., Supuran, C. T., Tars, K. (2015). X-ray crystallography-promoted drug design of carbonic anhydrase inhibitors. *Chemical Communications*, 51(33), 7108-7111.

Kannan, K., Ramanadham, M., Jones, T. (1984). Structure, refinement, and function of carbonic anhydrase isozymes: refinement of human carbonic anhydrase I. *Annals of the New York Academy of Sciences*, 429(1), 49-60.

Karagac, S. M., Yesilkent, E. N., Kizir, D., Ozturk, N., Isıyel, M., Karadas, H., Tosun, H., Karaman, M., Ceylan, H., Demir, Y. (2024). Esculetin improves inflammation of the kidney via gene expression against doxorubicin-induced nephrotoxicity in rats: *In vivo* and *in silico* studies. *Food Bioscience,* 62, 105159.

Kazi, I., Guha, S., & Sekar, G. (2017). CBr as a halogen bond donor catalyst for the selective activation of benzaldehydes to synthesize α,β-unsaturated ketones. *Organic Letters, 19*(5), 1244-1247.

Knopman, D. S., Amieva, H., Petersen, R. C., Chételat, G., Holtzman, D. M., Hyman, B. T., & Jones, D. T. (2021). Alzheimer disease. *Nature Reviews Disease Primers, 7*(33), 1-21.

Kocyigit, U. M., Budak, Y., Gurdere, M. B., et al. (2017). Synthesis, characterization, anticancer, antimicrobial and carbonic anhydrase inhibition profiles of novel (3aR,4S,7R,7aS)-2-(4-((E)-3-(3-aryl)acryloyl) phenyl)-3a,4,7,7a-tetrahydro-1H-4,7-methanoisoindole-1,3(2H)-dione derivatives. *Bioorganic Chemistry,* 70, 118-125.

Kryger, G., Silman, I., Sussman, J. L. (1999). Structure of acetylcholinesterase complexed with E2020 (Aricept®): implications for the design of new anti-Alzheimer drugs. *Structure*, 7(3), 297-307.

Kovar, S. E., Fourman, C., Kinstedt, C., Williams, B., Morris, C., Cho, K. J., & Ketcha, D. M. (2020). Chalcones bearing a 3,4,5-trimethoxyphenyl motif are capable of selectively inhibiting oncogenic K-Ras signaling. *Bioorganic & Medicinal Chemistry Letters, 30*(11), 127144.

Kumar, R., Sharma, P., Shard, A., Tewary, D. K., Nadda, G., & Sinha, A. K. (2012). Chalcones as promising pesticidal agents against diamondback moth (Plutella xylostella): microwave-assisted synthesis and structure-activity relationship. *Medicinal Chemistry Research, 21*(6), 922-931.

Le Duc, Y., Licsandru, E., Vullo, D., Barboiu, M., & Supuran, C. T. (2017). Carbonic anhydrases activation with 3-amino-1H-1,2,4-triazole-1-carboxamides: Discovery of subnanomolar isoform II activators. *Bioorganic & Medicinal Chemistry, 25*(5), 1681-1686.

Mahmudov, I., Demir, Y., Sert, Y., Abdullayev, Y., Sujayev, A., Alwasel, S. H., Gulcin, I. (2022). Synthesis and inhibition profiles of N-benzyl-and N-allyl aniline derivatives against carbonic anhydrase and acetylcholinesterase–A molecular docking study. *Arabian Journal of Chemistry*, 15(3), 103645

Mai, C. W., Yaeghoobi, M., Abd-Rahman, N., Kang, Y. B., & Pichika, M. R. (2014). Chalcones with electron-withdrawing and electron-donating substituents: Anticancer activity against TRAIL resistant cancer cells, structure-activity relationship analysis and regulation of apoptotic proteins. *European Journal of Medicinal Chemistry, 77*, 378-387.

Marucci, G., Buccioni, M., Dal Ben, D., Lambertucci, C., Volpini, R., & Amenta, F. (2021). Efficacy of acetylcholinesterase inhibitors in Alzheimer's disease. *Neuropharmacology, 1(190)*, 108352.

Mazumder, R., Ichudaule, Ghosh, A., Deb, S., & Ghosh, R. (2024). Significance of chalcone scaffolds in medicinal chemistry. *Topics in Current Chemistry, 382*(3), 22.

Meng, X. Y., Zhang, H. X., Mezei, M., Cui, M. (2011). Molecular docking: a powerful approach for structure-based drug discovery. *Current Computer-aided Drug Design,* 7(2), 146-157.

Mert, S., Demir, Y., Sert, Y., Kasımoğulları, R., Gulcin I. (2025). Synthesis, biological evaluation and molecular docking of novel pyrazole derivatives as multitarget acetylcholinesterase and carbonic anhydrase inhibitors. *Journal of Molecular Structure*, 1319, 139472.

Mikus, P., Krajciová, D., Mikulová, M., Horváth, B., Pecher, D., Garaj, V., & Supuran, C. T. (2018). Novel sulfonamides incorporating 1,3,5-triazine and amino acid structural motifs as inhibitors of the physiological carbonic anhydrase isozymes I, II and IV and tumor-associated isozyme IX. *Bioorganic Chemistry, 81*, 241-252.

Ouyang, Y., Li, J. J., Chen, X. Y., Fu, X. Y., Sun, S., & Wu, Q. (2021). Chalcone Derivatives: Role in Anticancer Therapy. *Biomolecules, 11*(6), 894.

Patil, P. S., Dharmaprakash, S. M., Ramakrishna, K., Fun, H. K., Kumar, R. S. S., & Rao, D. N. (2007). Second harmonic generation and crystal growth of new chalcone derivatives. *Journal of Crystal Growth, 303*(2), 520-524.

Petersen, R. C., Parisi, J. E., Dickson, D. W., Johnson, K. A., Knopman, D. S., Boeve, B. F., & Kokmen, E. (2006). Neuropathologic features of amnestic mild cognitive impairment. *Archives of Neurology, 63*(5), 665-672.

Petersen, R. C., Smith, G. E., Waring, S. C., Ivnik, R. J., Tangalos, E. G., & Kokmen, E. (1999). Mild cognitive impairment - Clinical characterization and outcome. *Archives of Neurology, 56*(3), 303-308.

Poyraz, S., Döndas, H. A., Yamali, C., Belveren, S., Demir, Y., Aydinoglu, S., & Sansano, J. M. (2024). Design, synthesis, biological evaluation and docking analysis of pyrrolidine-benzenesulfonamides as carbonic anhydrase or acetylcholinesterase inhibitors and antimicrobial agents. *Journal of Biomolecular Structure & Dynamics, 42*(7), 3441-3458.

Protein data Bank. https://www.rcsb.org/.

Raghavan, S., Manogaran, P., Kuppuswami, B. K., Venkatraman, G., & Narasimha, K. K. G. (2015). Synthesis and anticancer activity of chalcones derived from vanillin and isovanillin. *Medicinal Chemistry Research, 24*(12), 4157-4165.

Roman, B. I., De Ryck, T., Patronov, A., Slavov, S. H., Vanhoecke, B. W. A., Katritzky, A. R., & Stevens, C. V. (2015). 4-Fluoro-3′,4′,5′-trimethoxychalcone as a new anti-invasive agent. From discovery to initial validation in an metastasis model. *European Journal of Medicinal Chemistry, 101*, 627-639.

Russell, A. (1934). The constitution of tannins. Part I. Reduction products of chalkones and the synthesis of a typical phlobatannin. 218-221.

Scientific Software http://www.3dsbiovia.com/.

Schultze, S., & Grubmüller, H. (2021). Time-lagged independent component analysis of random walks and protein dynamics. *Journal of Chemical Theory and Computation, 17*(9), 5766-5776.

Schwartz, M. A., Rose, B. F., Holton, R. A., Scott, S. W., & Baburao, V. (1977). Intramolecular oxidative coupling of diphenolic, monophenolic, and nonphenolic substrates. *Journal of the American Chemical Society, 99*(8), 2571-2577.

Shibata, K., Katsuyama, I., Matsui, M., & Muramatsu, H. (1991). Synthesis of 3-cyano-2-methylpyridines substituted with heteroaromatics. *Journal of Heterocyclic Chemistry, 28*(1), 161-165.

Shinichi, I., Minako, S., & Ito, K. (1990). Polymer-supported poly(amino acids) as new asymmetric epoxidation catalyst of αß-unsaturated ketones. *Journal of Organic Chemistry, 55*(24), 6047-6049.

Supuran, C. T. (2008). Carbonic anhydrases: Novel therapeutic applications for inhibitors and activators. Nature Reviews: Drug Discovery, 7(2), 168–181

Taylor, R. D., Jewsbury, P. J., Essex, J. W. (2002). A review of protein-small molecule docking methods. *Journal of Computer-aided Molecular Design*, 16,151-166.

Temperini, C., Scozzafava, A., & Supuran, C. T. (2008). Carbonic anhydrase activation and the drug design. *Current Pharmaceutical Design, 14*(7), 708-715.

Tierney, M. C., Szalai, J. P., Snow, W. G., Fisher, R. H., Nores, A., Nadon, G., & StGeorgeHyslop, P. H. (1996). Prediction of probable Alzheimer's disease in memory-impaired patients: A prospective longitudinal study. *Neurology, 46*(3), 661-665.

Trott, O., Olson, A. J. (2010). AutoDock Vina: improving the speed and accuracy of docking with a new scoring function, efficient optimization, and multithreading, *Journal of Computational Chemistry*, 31(2), 455-461.

Tugrak, M., Gul, H. I., Akincioglu, H., & Gulcin, I. (2021a). New chalcone derivatives with pyrazole and sulfonamide pharmacophores as carbonic anhydrase inhibitors. *Letters in Drug Design and Discovery, 18*(2), 191-198.

Tugrak, M., Gul, H. I., Anil, B., & Gülçin, I. (2020). Synthesis and pharmacological effects of novel benzenesulfonamides carrying benzamide moiety as carbonic anhydrase and acetylcholinesterase inhibitors. Turkish Journal of Chemistry, 44(6), 1601.

Tugrak, M., Gul, H. I., Demir, Y., & Gulcin, I. (2021b). Synthesis of benzamide derivatives with thiourea-substituted benzenesulfonamides as carbonic anhydrase inhibitors. *Archiv Der Pharmazie, 354*(2).

Tugrak, M., Gul, H. I., Demir, Y., Levent, S., & Gulcin, I. (2021c). Synthesis and in vitro carbonic anhydrases and acetylcholinesterase inhibitory activities of novel imidazolinone-based benzenesulfonamides. *Archiv Der Pharmazie, 354*(4.

Tugrak, M., Gul, H. I., Sakagami, H., Gulcin, I., & Supuran, C. T. (2018). New azafluorenones with cytotoxic and carbonic anhydrase inhibitory properties: 2-Aryl-4-(4-hydroxyphenyl)-5-indeno[1,2-]pyridin-5-ones. *Bioorganic Chemistry, 81*, 433-439.

Tugrak, M., Gul, H. I., Sakagami, H., & Mete, E. (2017). Synthesis and anticancer properties of mono Mannich bases containing vanillin moiety. *Medicinal Chemistry Research, 26*(7), 1528-1534.

Tugrak, M., Yamali, C., Sakagami, H., & Gul, H. I. (2016). Synthesis of mono Mannich bases of 2-(4-hydroxybenzylidene)-2,3-dihydroinden-1-one and evaluation of their cytotoxicities. *Journal of Enzyme Inhibition and Medicinal Chemistry, 31*(5), 818-823.

Umesha, B., Basavaraju, Y. B., & Mahendra, C. (2015). Synthesis and biological screening of pyrazole moiety containing analogs of podophyllotoxin. *Medicinal Chemistry Research, 24*(1), 142-151.

Vaidya, S. S., Vinaya, H., & Mahajan, S. S. (2012). Microwave-assisted synthesis, pharmacological evaluation, and QSAR studies of 1,3-diaryl-2-propen-1-ones. *Medicinal Chemistry Research, 21*(12), 4311-4323.

Verpoorte, J. A., Mehta, S., Edsall, J. T. (1967). Esterase activities of human carbonic anhydrases B and C. The *Journal of Biological Chemistry,* 242(18), 4221-4229.

Wu, J. Z., Li, J. L., Cai, Y. P., Pan, Y., Ye, F. Q., Zhang, Y. L., & Liang, G. (2011). Evaluation and discovery of novel synthetic chalcone derivatives as anti-inflammatory agents. *Journal of Medicinal Chemistry, 54*(23), 8110-8123.

Yurt, B., Saglamtas, R., Demir, Y., İzol, E., Diril, H., Caglayan, C. (2024). Determination of in vitro antioxidant, anticholinergic, and antiepileptic activities of some medicinal and aromatic plant extracts. *KSU Journal of Agricalture and Nature,* 27, (Suppl. 1), 1-15.